Efficient, Accurate, and Rotation-invariant Iris Code

Naser Damer, Philipp Terhörst, Andreas Braun, Arjan Kuijper

***Abstract*—The large-scale of the recently demanded biometric systems has put a pressure on creating a more efficient, accurate, and private biometric solutions. Iris biometrics is one of the most distinctive and widely used biometric characteristics. High performing iris representations suffer from the curse of rotation inconsistency. This is usually solved by assuming a range of rotational errors and performing a number of comparisons over this range, which results in a high computational effort and limits indexing and template protection. This work presents a generic and parameter-free transformation of binary iris representation into a rotation-invariant space. The goal is to perform accurate and efficient comparison and enable further indexing and template protection deployment. The proposed approach was tested on a database of 10,000 subjects of the ISYN1 iris database generated by CASIA. Besides providing a compact and rotational-invariant representation, the proposed approach reduced the equal error rate by more than 55% and the computational time by a factor of up to 44 compared to the original representation.**

***Index Terms*—Biometrics, iris recognition, rotation-invariance.**

I. Introduction

The iris is a thin circular ring-shaped region positioned between the black pupil and the white sclera of the human eye. It is responsible for the amount of light reaching the retina by controlling the diameter of the pupil [1]. Essentially it consists of randomly generated characteristics that results in very complex and temporally constant patterns. Due to its rich texture information like spots, rifts, colors, filaments, minutia and other details it has about 10^{72} possible pattern [2]. This makes it very unique and generally results in one of the smallest false-matching rate of all biometric traits [3]. These properties make the iris an outstanding candidate for biometric recognition.

Different feature extraction approaches were previously proposed. The most widely used is the one proposed by Daugman [4]. A more recent feature extraction method is the ordinal measures proposed by Sun and Tan [5] aiming at being robust to image variations while maintaining high accuracy. These approaches, as many others, suffer from the sensitivity to eye tilt and thus not rotational-invariant. When performing comparison between a pair of iris feature vectors (codes), this rotation sensitivity is dealt with by performing multiple comparison between the vector pair at different shifts. This results in a high computational load, depending on the expected shift range and database size, especially when performing identification.

A compact, accurate, and rotation-invariant representation enables the development of advanced indexing, template protection, and fast search biometric solutions. Previous works tried to achieve this goal by extracting rotation-invariant features [6] or apply transformations [7]. However, these solutions suffered from low accuracy, computational complexity, or the requirement of parameter training.

This work presents a computationally efficient generic transformation into a rotational-invariant representation space of iris features while maintaining high accuracy. This was demonstrated by decreasing the equal error rate by a factor of 2 to 2.5 in comparison to the benchmark solution, while cutting the computational time by a factor of 14 to 44 in different settings.

In Section II a detailed look into related works is presented. Section III discusses the solution presented in this work. The experiment setup and the achieved results are detailed in Sections IV and V. Finally a conclusion is drawn in Section VI.

II. Related Work

One of the most widely used approaches to extract iris features is based on a method proposed by Daugman [4]. The iris is modeled with consideration to pupil dilatation, contraction, size inconsistencies and, non-concentric pupil displacement. However, it does not compensate rotational inconsistencies. The given iris is encoded using Gabor filters into a binary feature vector (iris code). These features have a virtually variable size for different iris images (because of the different region of interest defined by an image specific mask), which limits the possibilities of further transformations.

With a focus on robustness to intraclass variations and computational efficiency, Sun and Tan presented ordinal measures (OM) as a new type of iris features [5]. Ordinal measures describe a quality measurement related to the relative ordering of several quantities. Given two distinct image regions, the ordinal measure between these regions is encoded by the inequality of the average intensities. With multilobe differential filters (MLDFs) the OM features can additionally be extracted with flexible interlobe and intralobe parameters, such as location, scale (intra), orientation and distance (inter). The challenge still facing iris features such as OM is the rotation inconsistency of the resulting iris code. Ordinal measures feature extraction approach will be considered as a basis for the rotation-invariant representation presented in this work.

The discussed iris representations (codes) are sensitive to eye tilt and thus are not rotation-invariant. Therefore, to

This work was supported by the German Federal Ministry of Education and Research (BMBF) as well as by the Hessen State Ministry for Higher Education, Research and the Arts (HMWK) within CRISP.

N. Damer, P. Terhörst, A. Braun, and A. Kuijper are with the Fraunhofer Institute for Computer Graphics Research IGD, Darmstadt, Germany (e-mail: {naser.damer, philipp.terhoerst, andreas.braun, arjan.kuijper}@igd.fraunhofer.de).

P. Terhörst is also with the Physics Department, Technische Universität Darmstadt, Darmstadt, Germany.

A. Kuijper is also with the Mathematical and Applied Visual Computing Group, Technische Universität Darmstadt, Darmstadt, Germany.

compensate for that, comparison process usually includes shifting the templates against each others to calculate a distance (similarity) at different shifts. Based on the amount of shifts performed (usually limited to 7-8 bits [4][7]), this process amounts to a large number of comparison operations, especially in identification tasks.

Regarding previous attempts at rotation-invariant iris representation, some works focused on extracting rotation-invariant features from iris images [6][8]. Du et al. [6] calculated first moments of the iris line histograms to extract iris features. While Ives et al. [8] exploited iris histograms to extract rotational-invariant features. However, the performance of these approaches were unsatisfactory for realistic iris recognition implementations. Another feature extraction method focusing on the rotation-invariance property used a bank of non-separable orthogonal wavelet filters to capture iris details and then model the output as a fourth-order Gaussian Markov random field with its parameters forming the feature vector [9]. However, this approach requires parameter training as well as a large number of matrix multiplications.

Konrad et al. [10] aimed at reducing the computational costs of rotation-invariant iris recognition by using a serial classifier combination to join spatially-based rotation invariant iris recognition with local-feature based schemes. However, this approach might be effected by a changing database size and requires parameter tuning. A transformation approach based on bloom-filters was proposed by Rathgeb et al. [7] achieving good accuracy but faces the possibility of misalignment at filter block boundaries and requires parameter tuning.

In this work, different aspects of previous works are targeted by presenting a generic, accurate, and computationally efficient solution that requires no parametrization.

III. Rotation-invariant Representation

The ordinal measures offer properties including robustness, uniqueness and efficiency. However, the resulting iris codes suffer from rotation inconsistencies, which leads to heavy computational load when dealing with large databases. In this section, a rotation-invariant representation based on transforming ordinal measures is introduced to tackle this problem.

The transformation: initially, two basic transformations $\hat{\mathbf{u}}$ and $\hat{\mathbf{v}}$ are discussed. These transformations lead to the relative distance transformation $\mathbf{T}$ satisfying the claimed rotation-invariant property.

In order to discuss the basic transformations, it is essential to keep the following basic functions in mind. First of all, this section deals with a distance function within a given vector, called relative distance. This distance, $d(i,j)$, between the i^{th} and j^{th} location of a vector $\mathbf{v} \in \{0,1\}^n$ is defined as

$$d(i,j) = \min\left\{|i-j|, n-|i-j|\right\} \tag{1}$$

which considers the rotational property of iris codes.

The second important function for the transformation is the common Kronecker delta, which is used in two fashions.

$$\delta_{i,j} = \begin{cases} 1 & \text{if } i = j \\ 0 & \text{if } i \neq j \end{cases} \qquad \delta(n) = \begin{cases} 1 & \text{if } n = 0 \\ 0 & \text{if } n \neq 0 \end{cases} \tag{2}$$

The two basic transformations $\hat{\mathbf{u}}$**(v)** and $\hat{\mathbf{v}}$**(v)** already depict a solution to the above mentioned rotation problem. Given a binary iris code $\mathbf{v} \in \{0,1\}^n$ of length n, the functions $\hat{\mathbf{u}}$**(v)** and $\hat{\mathbf{v}}$**(v)** are called basic transformations of $\mathbf{v}$ and defined component-wise as follows:

$$\hat{u}_k(\mathbf{v}) = \sum_{i<j} \delta(d(i,j)-k)\, \delta_{v_i,0}\, \delta_{v_j,0} \tag{3}$$

$$= \sum_{\substack{i<j \\ v_i,v_j=0}} \delta(d(i,j)-k),\ \forall\ k \in \left\{1,2,\ldots,\left\lfloor \frac{n}{2} \right\rfloor\right\} \tag{4}$$

$$\hat{v}_k(\mathbf{v}) = \sum_{i<j} \delta(d(i,j)-k)\, \delta_{v_i,1}\, \delta_{v_j,1} \tag{5}$$

$$= \sum_{\substack{i<j \\ v_i,v_j=1}} \delta(d(i,j)-k),\ \forall\ k \in \left\{1,2,\ldots,\left\lfloor \frac{n}{2} \right\rfloor\right\} \tag{6}$$

It can easily be seen that $\hat{u}_k$ describes how many pairs of 0's have a distance of k, while $\hat{v}_k$ specifies the same for pairs of 1's. Furthermore, these transformations are static as they lost the property of rotation inconsistency due to the use of relative distances and histograms.

Even though each of the basic transformations alone performs poorly, which means that too much essential information is lost during the transformation, a simple linear combination offers the required properties for the biometric comparison task. Therefore, a transformation $\mathbf{T}(\mathbf{v})$ is defined as a linear combination of $\hat{\mathbf{u}}$ and $\hat{\mathbf{v}}$ and is given component-wise as

$$T_k(\mathbf{v}) = \hat{u}_k(\mathbf{v}) + \hat{v}_k(\mathbf{v}) = \sum_{i<j} \delta(d(i,j)-k)\ \delta_{v_i,v_j}. \tag{7}$$

Here, the k^{th} component of $\mathbf{T}(\mathbf{v})$ describes the number of same labeled pairs with a distance of k within $\mathbf{v}$. The result of this transformation $\mathbf{T}(\mathbf{v})$ is the proposed rotation-invariant representation and is noted here as RIR.

Error behavior: the reason behind the transformation success lies in its noise robustness. To understand this, the error behavior of each feature is analyzed in the following. The basic transformations in Equations 3 and 5 are rewritten as

$$\hat{u}_k(\mathbf{v}) = \sum_{\mathcal{N}_0} \delta(d(i,j)-k) \qquad |\mathcal{N}_0| = \binom{n_0}{2} \tag{8}$$

$$\hat{v}_k(\mathbf{v}) = \sum_{\mathcal{N}_1} \delta(d(i,j)-k) \qquad |\mathcal{N}_1| = \binom{n_1}{2} \tag{9}$$

with sums over $\mathcal{N}_0$ and $\mathcal{N}_1$ that describe sets of all locations pairs in $\mathbf{v}$, $\mathcal{N}_0$ is for pairs of 0's and $\mathcal{N}_1$ is for pairs of 1's. The cardinalities are given by binomial coefficients where n_0 and n_1 identify the number of 0's and 1's in $\mathbf{v}$. Considering the case in which some errors $|\mathbf{e}|$ are applied on $\mathbf{v}$, resulting in a vector $\mathbf{v}^e = \mathbf{v}+\mathbf{e}$, where $\mathbf{e} \in \{0,1\}^n$ is an error vector added in modulo-2 algorithmic. Furthermore, only two types of errors are assumed. Errors occurring only on 0's are denoted as $e_{0\to1}$ and errors on 1's are denoted as $e_{1\to0}$. The differences between

the basic transformations of $\mathbf{v}$ and $\mathbf{v}^e$ show the following properties

$$\Delta\hat{u}_k(\mathbf{v},\mathbf{v}^e) = \hat{u}_k(\mathbf{v}) - \hat{u}_k(\mathbf{v}^e) = \begin{cases} > 0 & \text{if } e_{0\to1} \\ < 0 & \text{if } e_{1\to0} \end{cases} \quad (10)$$

$$\Delta\hat{v}_k(\mathbf{v},\mathbf{v}^e) = \hat{v}_k(\mathbf{v}) - \hat{v}_k(\mathbf{v}^e) = \begin{cases} < 0 & \text{if } e_{0\to1} \\ > 0 & \text{if } e_{1\to0} \end{cases} \quad (11)$$

since $\delta(n) \geq 0$ and for the location pair sets of $\mathbf{v}^e$:

$$\text{if } e_{0\to1}: \quad |\mathcal{N}_0| > |\mathcal{N}_0^e|, \quad |\mathcal{N}_1| < |\mathcal{N}_1^e| \quad (12)$$

$$\text{if } e_{1\to0}: \quad |\mathcal{N}_0| < |\mathcal{N}_0^e|, \quad |\mathcal{N}_1| > |\mathcal{N}_1^e| \quad (13)$$

It can be observed that $\hat{\mathbf{v}}$ and $\hat{\mathbf{u}}$ behave completely antisymmetrical according to the different error types. For the assumption that the errors of the different types occur roughly the same number of times, the addition of the difference between the transformed vectors is small. Therefore, for $\hat{u} + \hat{v}$, there are less variations in each feature caused by errors.

$$\Delta\hat{u}_k(\mathbf{v},\mathbf{v}^e) + \Delta\hat{v}_k(\mathbf{v},\mathbf{v}^e) \approx 0 \quad (14)$$

Demonstrating error behavior: Figure 1 presents the error behavior of $\mathbf{T}(\mathbf{v})$. Here, $\|\mathbf{T}(\mathbf{v}) - \mathbf{T}(\mathbf{v}^e)\|_2$ was plotted over the number of errors $|\mathbf{e}|$. For each $|\mathbf{e}|$, a vector $\mathbf{v}$ was generated randomly and applied to get $\mathbf{v}^e$, then the L_2-distance is computed. This procedure was performed 200 times for each $|\mathbf{e}|$ value. In Figure 1, the dark line describes the mean of the distances while the shadowed area around it represents 95% of its variations. The same procedure was done for the basic transformations and the resulted error behavior is plotted in Figure 2.

In Figures 1 and 2, the problem facing the basic transformation can be seen. A certain L_2-distance in the basic transformation ($\hat{\mathbf{v}}$ or $\hat{\mathbf{u}}$) can correspond to a large range of errors. However, in the $\mathbf{T}(\mathbf{v})$ transformation, a certain distance points to a specific and relatively narrow range of errors and thus it is more informative for a comparison operation using distance calculations, such as required by biometric comparisons. However, the mentioned specific range can be seen on two ends of the plot. This is due to the fact that the $\mathbf{T}(\mathbf{v})$ transformation tends to be more similar when the number of errors in the original vector $|e|$ is far beyond $\frac{n}{2}$, because it just considers same labeled pairs but does not distinguish between them. However, this is irrelevant to iris comparison. 100 million OM features comparisons examined had a maximum of 470 iris code bits differences ($< \frac{n}{2}$), out of 1024 bits. These different bits corresponds in Figures 1 and 2 to the number of errors, and thus only the error range $[0, 512]$ is relevant here.

In the next section, deploying and evaluating the proposed transformation are discussed under different settings.

IV. Experimental Setup

This work utilized the ISYN1 iris synthetic images database [5][11][12][13][14] generated by CASIA [15] using its synthetic generator software [14]. In this work, 10,000 reference and 10,000 probe left iris images were used to evaluate the proposed approach.

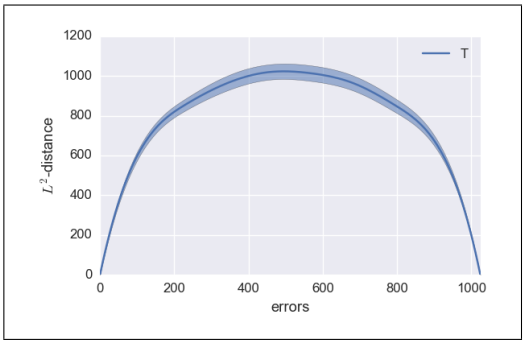

Fig. 1. Error behavior of $\mathbf{T}(\mathbf{v})$ transformation.

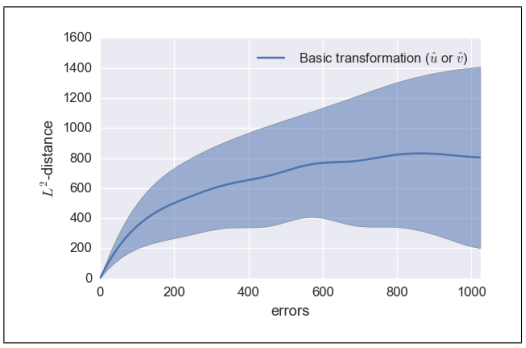

Fig. 2. Error behavior of basic transformation $\hat{\mathbf{u}}$ (or $\hat{\mathbf{v}}$).

From these images, the OM were extracted as described by Sun and Tan [5] with lobe size of 5x5 and σ=1.7. Furthermore, the rotation invariant transformation $\mathbf{T}$ (as described in Section III) was applied to generate a rotation invariant feature representation of the iris codes (RIR). In addition, each element in the RIR vectors was normalized using z-score normalization, so that each element has a zero mean and a variance of one.

Five different solutions were evaluated under a verification scenario. Two are based directly on OM features to benchmark the performance. The first does not consider the rotation-inconsistency properties of the features and only compare the iris codes using hamming distance (noted here as OM-HD). The other considers a minimum hamming distance over a shift range of 10 bits in both directions to capture most errors induced by the rotation invariance (noted here as OM-minHD10). The usually used shifting range is 7-8 bits [4], [7], however a shift range of 10 bits was considered here to capture a larger range of possible errors.

Another three solutions are based on our proposed RIR. Two are based on different distance measures between the RIR of the reference and the probe irises, Cosine similarity (RIR-Cosine) and Euclidean distance (RIR-L2). This aims at investigating the effect of different similarity measures. The third evaluated solution binarizes the RIR vectors and perform the comparison using hamming distance (BRIR-HD). The binarization is performed by threshold each feature value by its mean. It aims at creating even a more compact representation and allow for computationally light comparison.

Each of the five solutions was used to calculate a similarity score between every possible pair of the reference and probe irises. The resulted scores were analyzed to create a perfor-

mance comparison presented in the next section.

V. Results

The achieved results under different experiment settings are presented as receiver operating characteristic (ROC) curves and EER values. ROC curves plots the false acceptance rate (FAR) and the true acceptance rate (TAR) at different operational points (thresholds) and presents the tradeoff between the two rates. The EER is the common value of the false acceptance rate (FAR) and false rejection rate (FRR) at the operational point (decision threshold) where both rates are equal. In contrast to the ROC curves, which provides a wider insight into the verification performance at all possible operational points, the EER value provides a more general measure of the verification performance.

Figure 3 presents the ROC curves achieved by the different evaluated solutions. The OM-HD achieved a relatively much lower performance due to the rotation problem, and thus its relative curve lies much lower in the graph and would not appear in the plot at the presented ranges of interest. It is clear that the RIR-Cosine solution achieve the best performance with the highest TAR at the lowest FAR. This was followed by the BRIR-HD (with the lowest computational complexity) and RIR-L2. The benchmark OM-minHD10 achieved lower performance than the different evaluation settings related to our proposed RIR.

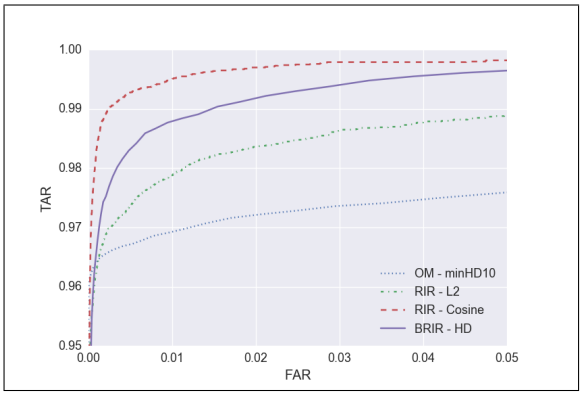

Fig. 3. ROC curves achieved by the different evaluated settings. The performance superiority of our proposed RIR approach is demonstrated.

Table I presents the EER values and computational time (per comparison) for each of the evaluation settings (running on an Intel®Core™i5-4590 3.30 GHz CPU). The enhancement in the EER values are clear in the solutions based on the proposed RIR. The very high EER achieved by the OM-HD setting is a clear representation of the rotation inconsistency problem.

The effect of the proposed RIR solution is clear both on the accuracy (EER) and computational complexity. Comparing the standard OM-minHD10 setting to the RIR-Cosine, the EER value drops by more than 2.5 times while the computational time required for a comparison is reduced by more than 14 folds. In the more efficient BRIR-HD setting, the computational time is reduced by a factor of 44 while reducing the EER to less than a half compared to the OM-minHD10.

Previous works focusing on feature extraction reported either low accuracy (EER>10% [8], 1-Rank IR<90% out of 105 irises [6]), or high comparison computation time (>4.5ms) [9]. To put our results in a broader prospective, a comparison is built between the effect (on accuracy and efficiency) of our proposed approach and the transformation approach based on bloom filters [7], which uses baseline features [16][17] of similar structure to OM. Table II lists the absolute values of the achieved EER of our most accurate and most efficient settings and the respective ones reported in [7]. However, to build a comparison, the reduction in the EER and comparison time with respect to the pre-transformation approaches (baseline) are reported. Our top accurate solution (RIR-Cosine) scores an EER of 23% of the pre-transformation (OM-minHD10) EER while reducing the comparison time to 6.56% of the pre-transformation time, these ratios were 95.8% and 23.56% respectively for the approach in [7]. The advantage of our proposed transformation is also clear when comparing the most efficient settings of both approaches.

TABLE I
Achieved EER and comparison computation time.

Evaluated solution	EER (%)	Comparison time (μs)
OM-HD	21.027	3.1
OM-minHD10	2.709	67.1
RIR-L2	1.730	4.7
RIR-Cosine	0.646	4.6
BRIR-HD	1.213	1.5

TABLE II
Comparison between the improvement induced by our approach and the Bloom-filter transformation [7].

Evaluated solution	Reported EER (%)	EER w.r.t. baseline (%)	Comparison time w.r.t baseline (%)
Bloom filter [7] (top accuracy)	1.14	95.80	23.57
Our approach (top accuracy)	0.646	23.85	6.56
Bloom filter [7] (top efficiency)	12.17	770.25	3.48
Our approach (top efficiency)	1.213	44.78	2.45

The proposed RIR transformation not only enhance the accuracy and computational efficiency, but also enables further solutions for iris database indexing and template protection because of its compact and rotation-invariant properties.

VI. Conclusion

Iris biometrics is one of the most accurate and widely used biometric characteristics on the large-scale. There is a need for a rotation-invariant iris representation that would allow for more efficient comparisons, besides enabling different indexing and template protection techniques. In response to this need, this work presented a generic and parameter-free transformation approach of binary iris code into a rotation-invariant space. This transformation was rationalized by discussing its behavior in response to simulated errors. The proposed rotation-invariant representation improved the original baseline solution by reducing the iris verification equal error rate by more than a half and the comparison computational time by a factor of 14 to 44 in different evaluation settings.

REFERENCES

[1] N. Poonguzhali and M. Ezhilarasan, "Iris indexing techniques: A review," *International Journal of Computer Applications*, vol. 73, no. 18, 2013.

[2] H. Proenca and L. A. Alexandre, "Toward noncooperative iris recognition: A classification approach using multiple signatures," *IEEE Trans. Pattern Anal. Mach. Intell.*, vol. 29, no. 4, pp. 607–612, Apr. 2007. [Online]. Available: http://dx.doi.org/10.1109/TPAMI.2007.1016

[3] L. C. S. Afonso, J. P. Papa, A. N. Marana, A. Poursaberi, and S. N. Yanushkevich, "A fast large scale iris database classification with optimum-path forest technique: A case study," in *The 2012 International Joint Conference on Neural Networks (IJCNN), Brisbane, Australia, June 10-15, 2012*, 2012, pp. 1–5. [Online]. Available: http://dx.doi.org/10.1109/IJCNN.2012.6252660

[4] J. Daugman, "How iris recognition works," *IEEE Transactions on Circuits and Systems for Video Technology*, vol. 14, no. 1, pp. 21–30, Jan 2004.

[5] Z. Sun and T. Tan, "Ordinal measures for iris recognition," *IEEE Trans. Pattern Anal. Mach. Intell.*, vol. 31, no. 12, pp. 2211–2226, 2009. [Online]. Available: http://dx.doi.org/10.1109/TPAMI.2008.240

[6] Y. Du, R. W. Ives, D. M. Etter, and T. B. Welch, "Use of one-dimensional iris signatures to rank iris pattern similarities," *Optical Engineering*, vol. 45, no. 3, pp. 037 201–037 201–10, 2006. [Online]. Available: http://dx.doi.org/10.1117/1.2181140

[7] C. Rathgeb, F. Breitinger, C. Busch, and H. Baier, "On application of bloom filters to iris biometrics," *IET Biometrics*, vol. 3, no. 4, pp. 207–218, 2014. [Online]. Available: http://dx.doi.org/10.1049/iet-bmt.2013.0049

[8] R. W. Ives, A. J. Guidry, and D. M. Etter, "Iris recognition using histogram analysis," in *Conference Record of the Thirty-Eighth Asilomar Conference on Signals, Systems and Computers, 2004.*, vol. 1, Nov 2004, pp. 562–566 Vol.1.

[9] J. Huang, X. You, Y. Yuan, F. Yang, and L. Lin, "Rotation invariant iris feature extraction using gaussian markov random fields with non-separable wavelet," *Neurocomput.*, vol. 73, no. 4-6, pp. 883–894, Jan. 2010. [Online]. Available: http://dx.doi.org/10.1016/j.neucom.2009.09.016

[10] M. Konrad, H. Stögner, A. Uhl, and P. Wild, "Computationally efficient serial combination of rotation-invariant and rotation compensating iris recognition algorithms," in *VISAPP 2010 - Proceedings of the Fifth International Conference on Computer Vision Theory and Applications, Angers, France, May 17-21, 2010 - Volume 1*, P. Richard and J. Braz, Eds. INSTICC Press, 2010, pp. 85–90.

[11] R. Cappelli, D. Maio, and D. Maltoni, "Synthetic fingerprint-database generation," in *Proceedings of the 16 th International Conference on Pattern Recognition (ICPR'02) Volume 3 - Volume 3*, ser. ICPR '02. Washington, DC, USA: IEEE Computer Society, 2002, pp. 30 744–. [Online]. Available: http://dl.acm.org/citation.cfm?id=839291.842894

[12] R. Cappelli, M. Ferrara, and D. Maltoni, "Minutia cylinder-code: A new representation and matching technique for fingerprint recognition," *IEEE Transactions on Pattern Analysis & Machine Intelligence*, vol. 32, pp. 2128–2141, 2010.

[13] R. Cappelli, M. Ferrara, D. Maltoni, and M. Tistarelli, "Mcc: A baseline algorithm for fingerprint verification in fvc-ongoing." in *ICARCV*. IEEE, 2010, pp. 19–23.

[14] Z. Wei, T. Tan, and Z. Sun, "Synthesis of large realistic iris databases using patch-based sampling," in *Pattern Recognition, 2008. ICPR 2008. 19th International Conference on*, Dec 2008, pp. 1–4.

[15] Chinese Academy of sciences, Institute of Automation, http://english.ia.cas.cn/, 2013.

[16] L. Ma, T. Tan, Y. Wang, and D. Zhang, "Efficient iris recognition by characterizing key local variations," *IEEE Transactions on Image Processing*, vol. 13, no. 6, pp. 739–750, June 2004.

[17] L. Masek, "Recognition of human iris patterns for biometric identification," Master's thesis, University of Western Australia, Australia, 2003.